



Contents lists available at SciVerse ScienceDirect

Earth and Planetary Science Letters

journal homepage: www.elsevier.com/locate/epsl

On the origin of the asthenosphere

Shun-ichiro Karato

Yale University, Department of Geology & Geophysics, New Haven, CT, USA

ARTICLE INFO

Article history:

Received 29 October 2011
 Received in revised form 19 December 2011
 Accepted 3 January 2012
 Available online xxxx

Editor: Y. Ricard

Keywords:

asthenosphere
 lithosphere
 partial melting
 water
 anelastic relaxation

ABSTRACT

Various models of the origin of the asthenosphere are reviewed based on the latest observations on mineral physics of mechanical properties, melting relationships and the thermal models of the upper mantle. Partial melting likely occurs throughout the upper mantle except for the lithosphere. However, in order to explain the inferred shallow lithosphere–asthenosphere boundary (LAB) with a large and sharp velocity reduction in the old oceanic mantle by partial melting, a high end of the geotherm and some mechanisms of melt accumulation are required. Purely thermal sub-solidus model of the asthenosphere is inconsistent with the sharp LAB. A sub-solidus model invoking a role of hydrogen content stratification explains the shallow and sharp LAB but it fails to explain a large velocity drop if the absorption band model of anelasticity is assumed. A review of recent literatures shows that grain-size sensitive anelastic relaxation inevitably has two successive processes, high-frequency elastically accommodated grain-boundary sliding followed by low-frequency diffusion-accommodated anelasticity. Anelastic relaxation caused by elastically accommodated grain-boundary sliding leads to a large velocity reduction (~5% or more). Assuming a plausible temperature and water content dependence of the peak frequency of this relaxation, it is shown that a substantial velocity reduction occurs at a nearly constant depth (~70 km) in the old oceanic region but at the age-dependent depth corresponding to the ~1300 K isotherm in the young oceans. This model also provides an explanation for the seismological observations on the cratonic upper mantle including the observed large velocity drop at the mid-lithosphere discontinuity and a small velocity change at the LAB. Implications for seismic anisotropy and for the geochemical characteristics of the asthenosphere are also discussed.

© 2012 Elsevier B.V. All rights reserved.

1. Introduction

The asthenosphere is a mechanically weak layer below the lithosphere (Barrell, 1914) characterized by low seismic wave velocities and high attenuation (e.g., Forsyth, 1975; Gutenberg, 1926; Shankland et al., 1981). The asthenosphere is considered to be the source region of mid-ocean ridge basalt, MORB (e.g., Hofmann, 1997; Stolper, 1980), and the production of MORB by partial melting is the largest volcanic activity on Earth. Consequently, there must be a close connection between mechanical weakness and partial melting, and the most popular model of the asthenosphere is to identify it with a layer where partial melting occurs (e.g., Anderson and Spetzler, 1970; Hirschmann, 2010; Lambert and Wyllie, 1970; Mierdel et al., 2007).

However, the connection between partial melting and mechanical weakness may not be direct. For instance, Stocker and Gordon (1975) pointed out that if the melt does not completely wet the grain-boundaries, then the influence of incipient melting on mechanical properties will be small. In fact, experimental studies on melting showed that most of the melts do not completely wet grain-boundaries of minerals under the shallow mantle conditions (Kohlstedt, 2002; Toramaru

and Fujii, 1986; Waff and Blau, 1979) and that the degree of partial melting in the asthenosphere away from mid-ocean ridges is small (~0.1% or less) (e.g., Hirschmann, 2010; Plank and Langmuir, 1992). Consequently, it is not clear if the onset of partial melting explains the seismological observations on the lithosphere–asthenosphere boundary (LAB).

Recent seismological observations amplify this point. Using high-resolution body wave techniques, some of the recent studies showed that the transition from the lithosphere to the asthenosphere (the lithosphere–asthenosphere boundary (LAB)) occurs at a shallow depth in the old oceanic mantle (~60 km in some regions) and the boundary is sharp and is associated with a large (5–10%) velocity drop (e.g., Gaherty et al., 1996; Kawakatsu et al., 2009; Kumar and Kawakatsu, 2011; Rychert and Shearer, 2009, 2011; Rychert et al., 2005; Schmerr, in press). It is not straightforward to explain such a large velocity drop at the relatively shallow depth in the old oceanic upper mantle. Similarly enigmatic is the frequently observed large velocity drop in the cratonic mantle at the depth of ~100–150 km much shallower than the expected depth of the LAB (Abt et al., 2010; Kumar et al., in press; Rychert and Shearer, 2009; Thybo, 2006; Thybo and Perchuc, 1997). There has been no widely accepted model for this mid-lithosphere discontinuity.

The purpose of this paper is to present a model that can explain most of these characteristics of the asthenosphere including geophysical and

E-mail address: shun-ichiro.karato@yale.edu.

geochemical characteristics based on the latest knowledge of physical properties of mantle materials. I will first review key observations and evaluate the previous models including models invoking partial melting and those where sub-solidus processes are considered. I will show that both partial melting model and the previously proposed sub-solidus model have serious difficulties in reconciling with the known material properties and the geothermal structures of the upper mantle. Then I will propose a new model in which the role of high-frequency grain-boundary sliding is emphasized. Finally, I will discuss the implications of the present model for a broad range of geophysical and geochemical observations.

2. Seismological observations on the asthenosphere

The asthenosphere is characterized by low seismic wave velocities and high attenuation, and by high electrical conductivity (Shankland et al., 1981). Explanation of high electrical conductivity was discussed in detail in the previous papers (Dai and Karato, 2009; Wang et al., 2006) and will not be repeated here. In this paper, I will focus on seismological aspects. Early surface wave studies showed that (i) there is a low velocity zone in the oceanic upper mantle at the depth range of ~50–200 km (depending on the age of the ocean floor) where the velocity drop from the lithosphere is ~5% (Forsyth, 1975; Montagner and Tanimoto, 1991; Nishimura and Forsyth, 1989), (ii) seismic wave attenuation is relatively high ($Q \sim 80$) compared to the lithosphere ($Q > 600$) (Dziewonski and Anderson, 1981; Yang et al., 2007), and (iii) there is significant seismic anisotropy in the upper mantle (Beghein and Trampert, 2004; Dziewonski and Anderson, 1981; Montagner and Tanimoto, 1991; Nettles and Dziewonski, 2008).

However, surface wave studies have only limited spatial resolution, and fine-scale structures have to be investigated using body waves with shorter wavelengths (Fischer et al., 2010; Kawakatsu et al., 2009; Kumar and Kawakatsu, 2011; Rychert and Shearer, 2009, 2011; Scherrer, in press). These studies showed that the lithosphere–asthenosphere boundary (the LAB) in the oceanic regions is sharp (less than ~10–15 km interval) at a depth of ~70 km (with some age dependence, e.g., Rychert and Shearer, 2011, as I will discuss later) and associated with a large velocity drop (5–10%).

Also, there is significant seismic anisotropy in the upper mantle. Global studies of seismic anisotropy using surface waves showed that the majority of the upper mantle has modest radial anisotropy characterized by $(V_{SH} - V_{SV})/V_S > 0$ (V_{SH} : velocity of horizontally polarized shear wave, V_{SV} : velocity of vertically polarized shear wave, V_S : average shear wave velocity) and the strength of radial anisotropy generally decreases with depth (Dziewonski and Anderson, 1981; Montagner and Tanimoto, 1991; Visser et al., 2008). Also there is azimuthal anisotropy, the fast direction being sub-parallel to the direction of material motion in most regions (Montagner and Tanimoto, 1991; Nishimura and Forsyth, 1989). However, a few important exceptions have also been noted. In some regions near subduction zone, the polarization direction of fast seismic waves is sub-parallel to trenches and nearly normal to the direction of flow inferred for a two dimensional trench subduction-induced flow (Long and Silver, 2009; Russo and Silver, 1994). Also there is exceptionally strong radial anisotropy in the asthenosphere of the central Pacific (Ekström and Dziewonski, 1998; Karato, 2008b), that affects the global model of radial anisotropy (Nettles and Dziewonski, 2008).

The situation is somewhat different for the continental upper mantle. In the continental upper mantle, seismological signature of a possible LAB (at ~200 km depth in the old continents) is weak (e.g., Abt et al., 2010; Eaton et al., 2009). Instead, there is a distinct velocity drop (from the shallow to the deep region) at around 100–150 km (Abt et al., 2010; Rychert and Shearer, 2009; Thybo, 2006; Thybo and Perchuc, 1997). Rychert and Shearer (2009) interpreted this as the LAB in the continents, but Abt et al. (2010), Thybo (2006), and Thybo and Perchuc (1997) considered that this is a mid-lithosphere discontinuity (MLD)

rather than the LAB. However, the origin and the significance of the MLD have not been well understood.

The essential features of the oceanic lithosphere–asthenosphere system are summarized in Fig. 1a and those of the continental upper mantle are shown in Fig. 1b. The seismological features that should be explained include (i) a sharp and large (5–10%) velocity drop at the oceanic LAB at ~70 km in the old oceanic regions, (ii) the orientation of seismic anisotropy that is sub-parallel to the plate motion with an exception in some subduction zones, (iii) the magnitude of anisotropy in the oceanic asthenosphere is less than a few % with some regional variations (Ekström and Dziewonski, 1998; Montagner and Tanimoto, 1991; Nettles and Dziewonski, 2008), (iv) a large velocity discontinuity at 100–150 km in the old continents, (v) a small velocity change at the continental LAB in the old continents, and (vi) trench parallel shear wave splitting below some subducting slabs (Long and Silver, 2009; Russo and Silver, 1994).

3. Materials science observations relevant to the asthenosphere

3.1. Partial melting

A popular model for the asthenosphere is to identify it with a layer of partial melting (e.g., Anderson and Spetzler, 1970; Hirschmann, 2010; Lambert and Wyllie, 1970; Mierdel et al., 2007). Melting relationship of upper mantle rocks has been studied in detail (e.g.,

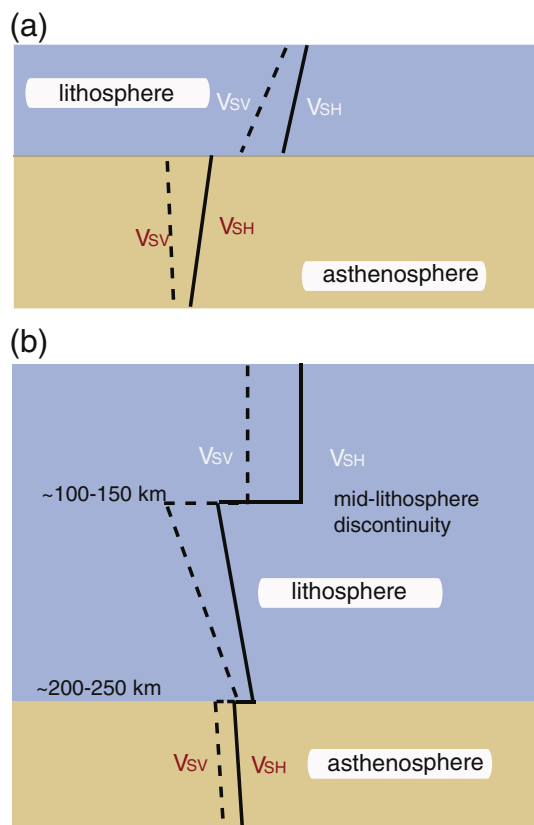


Fig. 1. Basic seismological observations of the upper mantle of Earth. (a) Oceanic upper mantle. At the LAB (lithosphere–asthenosphere boundary), there is a sharp and large drop in seismic wave velocity. The quality factor, Q , of the lithosphere is large (600 or higher), but the Q of the asthenosphere is smaller, ~80 (Dziewonski and Anderson, 1981). There is substantial anisotropy, both radial and azimuthal anisotropy, up to a few % with large regional variations (Dziewonski and Anderson, 1981; Ekström and Dziewonski, 1998; Montagner and Tanimoto, 1991; Nettles and Dziewonski, 2008). (b) Cratonic upper mantle. In the cratonic upper mantle, there is a distinct velocity drop at ~100–150 km and at the depth of ~200–250 km where the LAB is likely located, the seismic velocity changes only slightly (based on Abt et al., 2010; Nettles and Dziewonski, 2008).

Dasgupta and Hirschmann, 2007; Green et al., 2010; Hirschmann et al., 2009; Kushiro, 2001; Mierdel et al., 2007; Plank and Langmuir, 1992), and the following picture is well established (for a review see Hirschmann, 2010): below the mid-ocean ridges, hot materials ascend and the reduction of pressure leads to melting. Melting starts at ~100–150 km depth initially assisted by volatiles (water and/or carbon dioxide). The amount of melt produced in this stage is controlled by the amount of volatiles and is limited (less than ~0.1%). When materials reach ~70 km, melting occurs without the help of volatiles and the degree of melting increases substantially leading to the dehydration of residual minerals defining the chemically depleted lithosphere (e.g., Hirth and Kohlstedt, 1996; Karato, 1986; Karato and Jung, 1998).

Such a model implies that the degree of melting in the asthenosphere (~70 km or deeper) in regions away from mid-ocean ridges is small, and if melt migration is easy, the fraction of melt will also be small (e.g., Spiegelman and Elliott, 1993). The conditions for volatile-induced melting in these regions are largely controlled by the solubility contrast of volatiles between the melts and minerals, and recent experimental studies showed that an incipient melting (<0.1%) can occur at $T \sim 1300$ K and $P \sim 2\text{--}3$ GPa (e.g., Dasgupta and Hirschmann, 2007; Green et al., 2010; Mierdel and Keppler, 2004; Mierdel et al., 2007). Similarly, incipient melting also likely occurs in the upwelling materials at ~410-km if the water content in the transition zone exceeds ~0.05 wt.% (Hirschmann et al., 2009; Karato et al., 2007). Hirschmann (2006) estimated this to be ~0.4%, but later Hirschmann et al. (2009) corrected this to ~0.05%. Once partial melting occurs at ~410-km, the rest of the upwelling mantle materials will always be partially molten until they reach the bottom of the lithosphere (Karato, 2011). If the down-going flux is concentrated near subduction zones and the slow distributed upwelling currents occur in most of the mantle as proposed by Bercovici and Karato (2003), then most of the upper mantle materials are the residuals of a small degree of partial melting at ~410-km and hence is nearly homogenous and modestly depleted (Karato et al., 2006).

In summary, most of the upper mantle likely contains a small amount of melt except for the lithosphere where temperature is lower than the solidus, ~1300 K. However, the amount of melt expected from the melt generation rate and the velocity of melt migration is small (<0.1%) (e.g., Hirschmann, 2010; Spiegelman and Elliott, 1993), that leads to very small reduction in seismic wave velocities when melt does not completely wet grain-boundaries. Therefore, even if the presence of partial melting is assumed, it is necessary to invoke some mechanisms of melt accumulation in order to explain a large velocity reduction by partial melting. I will discuss this point later.

3.2. Mechanical properties

Mechanical properties such as the seismic wave velocities and seismic wave attenuation depend on temperature, pressure and composition. Among the compositional effects, the most important is the influence of water when we discuss the structure of the LAB. Temperature reduces seismic wave velocities and pressure increases the velocities. In the shallow part where the temperature gradient is high, temperature effect dominates and the velocities decrease with depth. In the deeper regions, temperature gradient becomes smaller and the pressure effect starts to dominate, leading to a minimum in seismic wave velocities.

The temperature and pressure dependence of seismic wave velocities has two components: anharmonic and anelastic effects (e.g., Karato, 1993). Water has only a weak effect on the anharmonic component (e.g., Jacobsen et al., 2008), whereas it likely has a large effect on the anelastic component (e.g., Aizawa et al., 2008; Karato, 2003; McCarthy et al., in press). The best-documented mechanism of anelastic relaxation is grain-boundary sliding accommodated by diffusional mass transport (Cooper, 2002; Jackson, 2009; Jackson et al., 2002). Both

experimental and theoretical studies have been conducted on this mechanism of anelastic relaxation. Theoretical studies on deformation of a polycrystalline material showed that the anelastic relaxation and long-term creep in a polycrystalline material occur as a successive process of elastically accommodated grain-boundary sliding followed by the accommodation due to diffusional mass transport (Ghahremani, 1980; Morris and Jackson, 2009; Raj and Ashby, 1971). Upon the application of an external stress, grain-boundary sliding occurs accommodated by elastic deformation that creates stress heterogeneity at grain-boundaries. The stress heterogeneity thus generated provides a driving force for diffusional mass transport. Diffusional mass transport, in turn, modifies the stress distribution and hence deformation by diffusional mass transport occurs initially as transient creep followed by steady state creep. Consequently, viewed in the frequency domain, anelastic behavior of a polycrystalline material contains a high-frequency peak of attenuation corresponding to the elastically accommodated grain-boundary sliding ($Q^{-1} \propto \frac{\omega\tau}{1+\omega^2\tau^2}$, Q^{-1} : seismic wave attenuation, ω : frequency, τ : relaxation time) followed by a distributed anelastic relaxation leading to power-law attenuation ($Q^{-1} \propto \omega^{-\alpha}$ with $\alpha = 0.1\text{--}0.3$) and finally the Maxwell body behavior ($Q^{-1} \propto \omega^{-1}$) (Fig. 2). Note that the amplitude of relaxation by elastically accommodated grain-boundary sliding can be large. Kê (1947) reported ~36% reduction in modulus in aluminum (~18% reduction in velocity), although later models (Ghahremani, 1980; Morris and Jackson, 2009) predict a small relaxation (~10% reduction in velocity or less).

Jackson and Faul (2010) and Sundberg and Cooper (2010) reported experimental observations on peridotites showing the above-mentioned behavior. Because most of seismological observations and high temperature anelasticity experiments show power-law behavior, the absorption band model is often used to characterize anelastic behavior of Earth's mantle (e.g., Karato (1993)). However, the model summarized above shows that in addition to the absorption band behavior, there must be a high frequency peak that causes a substantial velocity reduction. The characteristic frequency of grain-boundary relaxation increases with temperature (and likely with water content). If the characteristic frequency is higher than the seismic frequency band in the lithosphere but lower than the seismic frequency in the asthenosphere, then a substantial velocity drop occurs at the LAB. I will explore this possibility in the later part of this paper.

4. Models of the LAB

Mechanical strength of minerals is reduced at high temperatures including both elastic and plastic properties (e.g., Karato, 2008a). Consequently, several studies examined the effects of high temperature on the mechanical properties (particularly seismic wave velocities and attenuation) (e.g., Faul and Jackson, 2005; Schubert et al., 1976; Stixrude and Lithgow-Bertelloni, 2005). However, a purely thermal model predicts only a diffuse LAB that is inconsistent with the recent seismological studies showing a sharp transition. Therefore, one needs something else to explain the sharp and large change in seismic wave velocity at the LAB.

4.1. Partial melt models

A classic model for the asthenosphere is to identify it with a layer where incipient partial melting occurs (Anderson and Spetzler, 1970; Lambert and Wyllie, 1970). If partial melting occurs at the LAB and if partial melting reduces the seismic wave velocities substantially, then such a model would explain a sharp and a large velocity drop at the LAB.

However, such a model has two difficulties in view of the recent studies on materials properties and seismological observations. First, although recent petrological studies showed that some partial

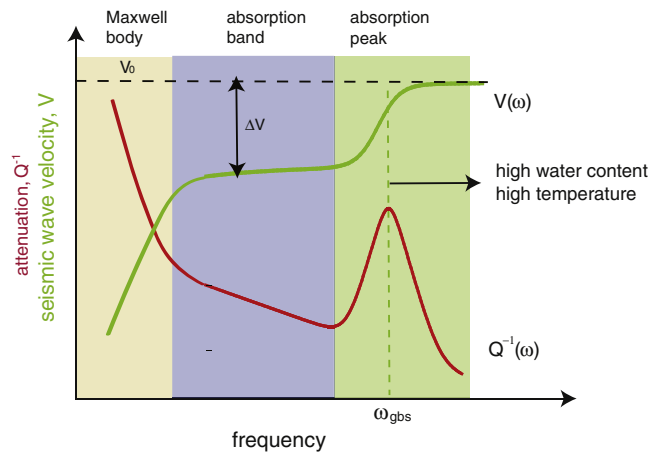


Fig. 2. A schematic diagram showing the variation of seismic wave velocity and attenuation with frequency (based on Morris and Jackson, 2009). At high frequency, anelastic relaxation occurs by elastically accommodated grain-boundary sliding. Anelasticity by this mechanism is characterized by a sharp peak at ω_{gbs} followed by (in the lower frequencies) diffuse absorption band due to diffusional accommodation. Finally, material behavior changes to the Maxwell body behavior. ω_{gbs} increases with water content and temperature. In the lithosphere $\omega_{seismic} > \omega_{gbs}$ ($\omega_{seismic}$: seismic frequency) and the velocity is unrelaxed velocity (high asymptotic velocity), whereas in the asthenosphere, $\omega_{seismic} < \omega_{gbs}$ and the velocity is relaxed velocity.

melting can occur in the asthenosphere away from the ridge caused by the presence of water and/or carbon dioxide (e.g., Green et al., 2010; Hirschmann, 2010; Mierdel et al., 2007), this occurs only when temperature exceeds ~ 1300 K (at the pressure of ~ 2 – 3 GPa). Recent body-wave seismological studies showed that the depth of the LAB in the old (~ 120 Myrs) oceanic upper mantle is at ~ 60 km in some regions (e.g., Kumar and Kawakatsu, 2011; Schmerr, in press). Using a standard geothermal model of the oceanic upper mantle, the temperature at the depth of 60 km will be 900–1200 K for the age of 120 Myrs (e.g., Davies, 1988; McKenzie et al., 2005; Ritzwoller et al., 2004). Because ~ 1300 K is needed for partial melting, one needs to choose an exceptionally hot model such as the one by Stein and Stein (1992) to explain partial melting at ~ 60 km in the old oceans. However, Stein and Stein (1992) assumes the potential temperature of ~ 1680 K that is too high to be consistent with the thickness of the oceanic crust (McKenzie and Bickle, 1988). McKenzie et al. (2005) presented a modified model consistent with the crustal thickness, heat flow and the bathymetry in which the temperature at 60 km in the old oceanic mantle is ~ 1000 K far below the solidus. So I conclude that partial melting at ~ 60 km in the old oceanic mantle is difficult, if not impossible, to reconcile with geothermal models of the oceanic mantle.

Also, even if there is partial melting, the amount of melt in the old asthenosphere is limited by the available volatile components and is less than $\sim 0.1\%$ if there is no melt accumulation (e.g., Hirschmann, 2010; Plank and Langmuir, 1992). Because melts do not completely wet grain-boundaries under the shallow asthenosphere conditions, the influence of a small amount of partial melting on mechanical properties is only modest and cannot explain a large velocity drop (Kohlstedt, 2002; Takei, 2002) (see also Jackson et al., 2004; McCarthy et al., in press). Therefore in order to explain the observed large velocity drop at the oceanic LAB, one needs to invoke some specific mechanisms to increase the melt fraction.

Kawakatsu et al. (2009) presented one of such models motivated by the experimental study by Holtzman et al. (2003) who showed that a layered structure is developed in a partially molten material by shear deformation including the layers of high melt fraction. In Kawakatsu et al.'s (2009) model, the net melt fraction is small ($< 1\%$) but seismic wave velocity in the melt-rich layer is assumed to be very low (by several 10s of %) that results in a reduced SV (vertically

polarized S wave) velocity. However, the stability of such a structure is questionable from the geodynamic point of view. First, according to Holtzman et al. (2003), the melt-rich layers formed by deformation is tilted by $\sim 20^\circ$ from the shear plane. If the melt-rich layer is tilted, then gravity will drain the melt and it is difficult to maintain such a melt-rich layer for a geological time due to efficient compaction (e.g., Ribe, 1985). Furthermore, Hernlund et al. (2008a, 2008b) showed that if such a melt-rich layer is present there will be gravitational instability to destroy it. In addition, in the model by Kawakatsu et al. (2009), the velocity drop is attributed to SH/SV shear wave anisotropy. Consequently, the magnitude of velocity drop must be equal to the magnitude of radial anisotropy ($(V_{SH} - V_{SV})/V_S = 5$ – 10%). Although relatively large radial anisotropy is reported in the central Pacific (Ekström and Dziewonski, 1998; Nettles and Dziewonski, 2008), the magnitude of radial anisotropy is in most cases less than a few % (Beghein et al., 2006; Montagner and Tanimoto, 1990, 1991; Nishimura and Forsyth, 1989) that is smaller than the velocity drop at the oceanic LAB (5–10%, Kawakatsu et al., 2009; Rychert and Shearer, 2009, 2011; Rychert et al., 2005). Furthermore, if one uses the model by Holtzman et al. (2003) on the structure of sheared partially molten peridotite, the direction of azimuthal anisotropy caused by olivine lattice-preferred orientation is orthogonal to the direction of flow, that is inconsistent with most of the seismological observations (e.g., Montagner and Tanimoto, 1990, 1991; Nishimura and Forsyth, 1989). I conclude that the explanation of the sharp and large velocity drop at the LAB by the presence of a layered structure in the asthenosphere is difficult to be consistent with seismological observations and the presence of such a structure is questionable from the geodynamic point of view.

An alternative model is to assume that the LAB may correspond to the depth at which melt accumulates due to the permeability barrier (e.g., Hirschmann, 2010; Parmentier, personal communication in 2011). The permeability barrier corresponds to the depth at which geotherm coincides with the solidus. The solidus temperatures corresponding to water and/or carbon dioxide assisted melting is ~ 1300 K, and such a high temperature at ~ 60 km in the old oceanic mantle is difficult as discussed before. Furthermore, the structure of such a layer depends on the melt supply rate and the compaction length (that depends on the permeability, solid and melt viscosity) and it is not clear if such a layer can explain the observed seismic velocity (I will come back to this point when I discuss the possible role of such a layer to lubricate the lithosphere–asthenosphere boundary). Therefore, I will explore sub-solidus models to explain the observed seismological structure of the LAB.

4.2. Sub-solidus models

In order to explain sharp velocity drop by a sub-solidus model, factors other than temperature need to be invoked. Faul and Jackson (2005) emphasized the role of grain-size. In their formulation, unrelaxed velocity is grain-size dependent (their equation (7)). Consequently, if there is a large reduction in grain-size across the LAB (larger in the lithosphere), one might explain a sharp and large velocity drop even if $Q \sim 80$ or so. However, not only there are no physically plausible mechanisms to cause such a change in grain-size (only a small grain-size variation is observed in the typical upper mantle; Avé Lallemant et al., 1980; Karato, 1984) but also the formula (their equation (7)) that they used has a weak physical basis. Unrelaxed velocity in their model corresponds to the velocity affected by a high-frequency relaxation, and the theoretical models reviewed in the previous section (see also Supplemental Materials I) show that the unrelaxed velocity is independent of grain-size although the characteristic frequency of grain-boundary sliding is grain-size dependent. If physically appropriate formula is used and geologically observed range of grain-size in the upper mantle is used, then the velocity would change only by $\sim 0.2\%$ or less. Therefore, I conclude that this model is not viable.

Karato and Jung (1998) proposed a model in which a sharp drop in velocity occurs by a sharp increase in the water content below ~70 (± 10) km. Due to partial melting at mid-ocean ridges, the hydrogen content in the oceanic upper mantle changes drastically at ~70 km and therefore the LAB depth is relatively insensitive to the age of the ocean floor, which is consistent with the latest observations (Kumar and Kawakatsu, 2011; Rychert and Shearer, 2009). However, Karato and Jung (1998) assumed an absorption band model where the velocity drop and the seismic attenuation are directly connected (Anderson and Given, 1982) and therefore with $Q \sim 80$ in the asthenosphere, that model predicts only a small velocity drop (<1%). Yang et al. (2007) noted, however, that the amount of velocity reduction in the asthenosphere (~5–10%) is much higher than expected from attenuation ($Q \sim 50$ –100) assuming the absorption band model (see also Karato, 1977). This suggests that there is an absorption peak (or peaks) at the frequency higher than seismic frequency that causes velocity reduction but does not contribute to attenuation in the asthenosphere.

The physical models for the presence of a high-frequency peak were discussed in the previous section (Section 3.2). In order to calculate the variation in the relaxation peak, I use the results reported by Jackson and Faul (2010) that showed the high-frequency peak. Sundberg and Cooper (2010) found a tail of the high-frequency peak but the peak was not clearly identified, although their results are similar to those by Jackson and Faul (2010). Jackson and Faul (2010) found a relaxation peak (at 1 Hz) at $T \sim 1300$ K for 1 mm grain-size (for nearly water-free samples). This implies that if temperature is less than ~1200 K and no water is present, materials should have unrelaxed velocities, whereas if temperature is higher or with a higher water content, materials should show relaxed velocities (addition of water enhances all the known transport properties of olivine and other silicates (e.g., Karato, 2008a) and I assume that grain-boundary sliding is enhanced by

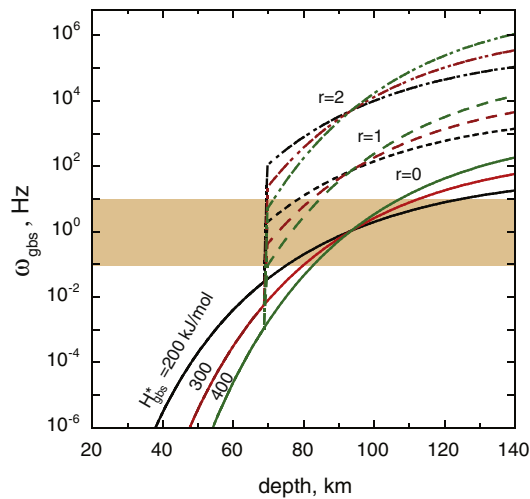


Fig. 3. Depth variation of the characteristic frequency of grain-boundary relaxation, ω_{gbs} . The relation $\frac{\omega_{gbs}(T, C_W)}{\omega_{gbs}(T_0, C_W^0)} = \left(\frac{C_W}{C_W^0}\right)^r \exp\left[-\frac{H_{gbs}^*}{RT_0} \left(\frac{T_0}{T} - 1\right)\right]$ is used (ω_{gbs} : characteristic frequency of grain-boundary sliding, T : temperature, T_0 : reference temperature (= 1300 K), C_W : water content (water content in the deep asthenosphere is assumed to be $\sim 10^{-2}$ wt.%), C_W^0 : reference water content (= 10^{-4} wt.%), r : a non-dimensional constant, H_{gbs}^* : activation enthalpy for grain-boundary sliding (the reference frequency, $\omega_{gbs}(T_0, C_W^0)$, is 1 Hz; Jackson and Faul, 2010) (for details see Supplemental Materials I). $H_{gbs}^* = 200, 300,$ and 400 kJ/mol and $r = 0, 1$ and 2 are used (from the experimental studies on grain-boundary properties, it is expected that $r > 1$ ($r = 0$ corresponds to a case of no water effect)). The geotherm corresponding to the 100 Myrs old oceanic mantle and the water content versus depth curve calculated by Karato and Jung (1998) are used. The shaded region indicates the frequency of typical body waves (~ 1 Hz). The increase in the characteristic frequency with depth is gradual if there is no influence of water ($r = 0$). However, if there is substantial effect of water ($r > 1$), then the characteristic frequency changes rapidly at ~ 70 km where a large change in water content occurs.

water; see Supplemental Materials I for details). At the LAB (60–80 km) in the old oceanic mantle, temperature is ~ 900 –1200 K. Also below ~ 70 km, both temperature and water content are higher (Hirth and Kohlstedt, 1996; Karato and Jung, 1998), and therefore, the seismic wave velocity in a layer below ~ 70 km should be low by several %. This can be seen from Fig. 3 where I plot the characteristic frequency of the high-frequency peak for the range of activation enthalpy and water content sensitivity (for details see Supplemental Materials I). For most of water-sensitive models, the transition from unrelaxed to relaxed state occurs sharply (with a width less than 10 km) at around ~ 70 km, although the transition is diffuse if water effect is not included. Corresponding velocity-depth profiles for the oceanic upper mantle for this model are shown in Fig. 4. This model also predicts anisotropic structures that are consistent with seismological observations (Karato et al., 2008).

Note that this model predicts age-dependent LAB in the young ocean where the LAB is shallower than ~ 70 km. In the young ocean, the temperature of ~ 1300 K will occur at a depth shallower than ~ 70 km where materials are water-poor. Consequently, the LAB depth in the young oceanic regions is age-dependent until this depth becomes ~ 70 km (at the age of 40–80 Myrs dependent on the model of geotherm). The age dependence of the oceanic LAB predicted from this model is shown in Fig. 5. Note that the shallow LAB in the young ocean predicted by this model occurs due to the temperature-induced high frequency relaxation, and therefore the boundary should be relatively diffuse (the transition from the lithosphere to the asthenosphere will occur for ~ 10 –20 km depth range dependent on the geothermal gradient).

This model also predicts seismic velocity structure of the continental upper mantle that can be compared with the available observations (Fig. 1b). According to the present model, a substantial velocity drop occurs at temperatures of ~ 1300 K (under dry conditions). Temperature of ~ 1300 K would correspond to a depth of ~ 100 –150 km in the typical old continental upper mantle (e.g., Artemieva, 2009). Therefore it is

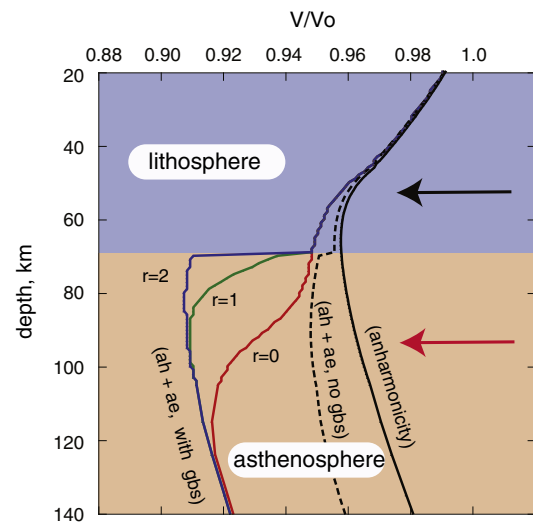


Fig. 4. Seismic wave velocity versus depth profiles in the upper mantle (100 Myrs old oceanic geotherm (half-space cooling model is assumed)). A black curve (anharmonicity): a model with only the effect of anharmonicity is considered. A broken black curve: a model by Karato and Jung (1998) (absorption band model). A solid blue curve: a model with grain-boundary sliding ($r = 2$). A solid green curve: a model with grain-boundary sliding ($r = 1$). A solid red curve: a model with grain-boundary sliding ($r = 0$ (no water effect)). A sharp and large velocity drop at ~ 70 km can be explained when the influence of grain-boundary sliding is included with some sensitivity to water ($r = 1$ –2). In addition to the depth variation in velocity, substantial anisotropy exists in the upper mantle. Only azimuthal anisotropy is shown. A black arrow shows the direction of plate motion, and a red arrow shows the direction of the fast waves in this model. Radial anisotropy predicted by this model is $(V_{SH} - V_{SV})/V_S \sim 2$ –5% (Karato et al., 2008). (For interpretation of the references to color in this figure legend, the reader is referred to the web version of this article.)

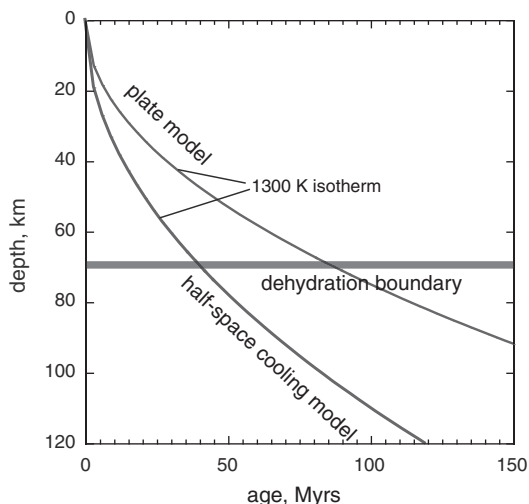


Fig. 5. The age dependence of the oceanic LAB predicted by the present model. In the young ocean (say less than ~ 50 Myrs), the LAB is relatively diffuse and age-dependent following roughly the isotherm of $T \sim 1300$ K. When this isotherm becomes ~ 70 km depth, then the LAB will be age independent and remains at ~ 70 km. In this regime, the LAB is controlled by the contrast in the water content and will be sharper.

tempting to suggest that the mid-lithosphere discontinuity observed in many continental upper mantle at this depth range may be caused by grain-boundary relaxation. In this model, the regional variation in the depth of MLD would correspond to the regional variation in the geotherm. Another implication is the seismic signal from the continental LAB. The LAB in the cratonic regions is likely a rheological boundary at a depth ~ 200 km or deeper across which viscosity changes significantly (e.g., Karato, 2010; Lenardic and Moresi, 1999). Most likely cause for the viscosity contrast is the contrast in the water content (Karato, 2010). However, the change in the water content at the continental LAB will not cause a large velocity reduction, because the temperature at the continental LAB likely exceeds the characteristic temperature of grain-boundary relaxation and hence materials there will follow the absorption band model behavior where the velocity reduction is limited by the Q value (less than 1%).

5. Discussions

5.1. Geochemical implications

Let us now discuss models to explain the geochemical characteristics of the asthenosphere. The cause of depletion in incompatible elements is often attributed to partial melting associated with the continental crust formation in the Archean (~ 3 Gyrs ago) (Hofmann, 1988) (for a more recent review see Hofmann, 2004). Indeed, the abundance pattern of trace elements of MORB is complementary to that of the continental crust that formed the basis of this model. However, this model has a difficulty from the geodynamic point of view. The residue of partial melting associated with the continental crust formation is highly depleted peridotites similar to those of the continental lithosphere (Carlson et al., 2005). In order to explain only modest depletion of the source region of MORB (the asthenosphere), highly depleted materials need to be mixed well with less-depleted (unprocessed) materials in the upper mantle to make modestly depleted and homogeneous asthenosphere (Hofmann, 1988). However, efficient mixing of highly depleted and undepleted materials in the upper mantle is difficult because these two components have a large viscosity contrast (Karato, 2010; Manga, 1996) (a factor of $\sim 10^3$). For good mixing, several components in a mixture must deform to large strains (> 10) (Ottino, 1989). For a typical strain-rate of 10^{-15} s^{-1} , strain of $\sim 10^2$ can be accumulated for the age of Earth. However, strain in the depleted component is less

than the average strain and is ~ 0.1 for the viscosity contrast of $\sim 10^3$. Indeed, the survival of the deep continental roots for a few billions of years is considered to be the result of a large viscosity contrast (Karato, 2010). Therefore this model unlikely explains the nearly homogeneous composition of the asthenosphere.

An alternative, and physically more plausible model for the generation of the homogeneous, modestly depleted asthenosphere, is that the asthenosphere is a residue of a small degree of melting at 410 km (Bercovici and Karato, 2003; Karato et al., 2006). Evidence of melting near 410 km has been obtained by seismological studies (Tauzin et al., 2010) showing low velocity regions above 410 km (see also the inference of 410-km melting from electrical conductivity observations, Karato, 2011). The composition of the residual materials after partial melting is controlled by the chemical composition along the solidus, and remains nearly homogeneous even though the composition of the materials before melting may vary. The degree of depletion by the melting at 410 km is modest because the degree of melting at 410 km is expected to be small (Karato et al., 2006) (~ 0.1 – 1%). The water content of the asthenosphere in this model is estimated to be ~ 0.01 wt.% (Karato et al., 2006) that is consistent with other estimates (Dai and Karato, 2009; Hirschmann, 2010). All of these predictions of the model agree with the chemical characteristics of the asthenosphere.

5.2. Possible interpretation of trench parallel flow below the slabs

The melt produced at 410 km will go down to the 410-km discontinuity in the deep region where the melt density is larger than the density of minerals (Karato et al., 2006). However, at a shallow depth, the melt density must be lower than those of co-existing minerals. Consequently, some melt must rise in the shallow upper mantle. If extensional stress exists, such a melt may rise to form “petit-spots” (Hirano et al., 2007). When these melts reach the bottom of the lithosphere, they will be frozen to form a thin water-rich gabbroic layer (Fig. 6). The thickness of this layer depends on the melt production rate and the age of the lithosphere, and is estimated to be ~ 0.1 – 1 km for ~ 0.1 – 1% partial melting at the age of ~ 100 Myrs (Supplemental Materials II). Because water-rich gabbro has much lower creep resistance than peridotites (e.g., Caristan, 1982; Chen et al., 2006), this layer has significantly smaller viscosity than the layers below and above and hence will act to decouple the lithosphere motion from the asthenospheric motion. Consequently, if there is substantial trench migration, then trench parallel flow may develop and this provides a mechanism to explain trench parallel flow beneath subducted lithosphere inferred from seismic anisotropy (Long and Silver, 2009).

6. Summary and concluding remarks

In the previous studies, the sharp LAB was attributed either to the presence of partial melt (Hirschmann, 2010; Kawakatsu et al., 2009) or to the weakening by water (hydrogen) assuming the absorption band model (Karato and Jung, 1998). Both models have difficulties in explaining a range of seismological observations including the magnitude of velocity drop and the nature of anisotropy simultaneously. A modified version of sub-solidus model is presented in which the role of water (hydrogen) to weaken the grain-boundaries is proposed to cause a sharp and large velocity reduction, although the cause for the transition from unrelaxed to relaxed velocity at the LAB in the young oceanic mantle is due to temperature. A large velocity reduction in the mid-lithospheric depth in the old continents is likely due to the same mechanism. This sub-solidus model also provides a natural explanation for the nature of seismic anisotropy in the asthenosphere including the plate parallel anisotropy in most of the asthenosphere and the trench parallel shear wave splitting observed below some slabs.

A classic model to explain homogeneous and modestly depleted asthenosphere is to presume well mixing of highly depleted residue

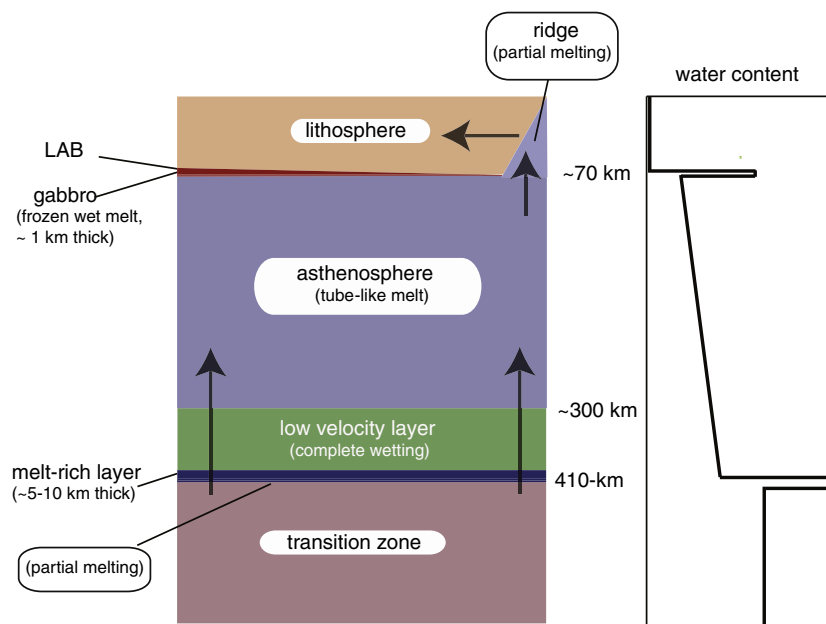


Fig. 6. A schematic diagram showing the structure and processes affecting the nature of the asthenosphere (the water content–depth profile is based on Karato (2011) and is only schematic). A low degree of partial melting occurs at ~410 km due to high water content in the transition zone. The asthenosphere is a residual of this partial melting and contains ~0.01 wt.% (depending on the depth) of water that is enough to make it soft. Beneath the ridge, extensive partial melting occurs at ~70 km (Hirth and Kohlstedt, 1996) that forms highly depleted lithosphere defining the lithosphere–asthenosphere boundary at ~70 km. In the deep upper mantle (~300 km or deeper), a small amount of melt completely wets olivine grain-boundaries (Yoshino et al., 2007) causing a thick low velocity regions above 410 km (Tauzin et al., 2010). Near the 410-km discontinuity, melt is likely denser than the surrounding minerals (Karato et al., 2006), and stays at 410 km or in the deep mantle (Bercovici and Karato, 2003). However, melt becomes buoyant at a shallower depth, and will rise to the bottom of the lithosphere, providing an explanation for “petit spots” (Hirano et al., 2007) and the lubrication needed to explain the trench parallel anisotropy (Long and Silver, 2009) (Supplemental Materials II).

of continental crust formation and less depleted primitive materials (Hofmann, 1988). Recognizing the geodynamical difficulty, an alternative model is proposed in which the modestly depleted and homogeneous composition of the asthenosphere is attributed to a small degree of partial melting at 410 km. This model implies that most part of the upper mantle (except for the lithosphere) is partially molten. However, in most of the shallow asthenosphere, partial melting does not result in large changes in seismic wave velocities because the melt fraction is low and melt wets only a small fraction of grain-boundaries. In contrast, partial melting results in a large velocity drop in the deep upper mantle where melt likely wets olivine grain boundaries completely (Yoshino et al., 2007). This provides an explanation for a thick low velocity layer above 410 km (Tauzin et al., 2010).

In the present model of the asthenosphere, water plays an essential role. Partial melting contributes to define the asthenosphere by redistributing water but it does not directly affect the properties so much. Water-induced melting at 410 km results in modestly depleted asthenosphere that still contains ~0.01 wt.% of water that is enough to weaken these materials. Below mid-ocean ridges, a high degree of partial melting occurs and most of water is removed to define a sharp LAB at ~70 km depth. The remaining uncertainties in this model include the degree of grain-boundary weakening by water (hydrogen) and the precise depth at which complete wetting of grain-boundaries by melt occurs. Further experimental studies on these issues are needed to understand the nature of the asthenosphere. Also improved seismological studies on the sharpness (its age dependence) of the LAB will be helpful to discriminate several competing models.

Acknowledgments

This study is partly supported by the grants from National Science Foundation. The author acknowledges discussions with Ian Jackson, Stephen Morris, Yasuko Takei and Slava Solomatov on anelasticity, John Hernlund for the instability of a partial melt layer, Jean-Paul Montagner, Hitoshi Kawakatsu, Maureen Long and Jeffrey Park on the

seismological aspects, and Karl Turekian for the geochemical aspects. Ian Jackson, Yanick Ricard and Yasuko Takei provided helpful reviews. Nick Schmerr and Rainer Kind kindly provided preprints of their papers.

Appendix A. Supplementary data

Supplementary data to this article can be found online at doi:10.1016/j.epsl.2012.01.001.

References

- Abt, D.L., Fischer, K.M., French, S.W., Ford, H.A., Yuan, H., Romanowicz, B., 2010. North American lithosphere discontinuity structure imaged by P_s and S_p receiver functions. *J. Geophys. Res.* 115. doi:10.1029/2009JB006691.
- Aizawa, Y., Barnhoorn, A., Faul, U.H., Fitz Gerald, J.D., Jackson, I., Kovács, I., 2008. Seismic properties of Anita Bay dunite: an exploratory study of the influence of water. *J. Petrol.* 49, 841–855.
- Anderson, D.L., Given, J.W., 1982. Absorption band Q model for the Earth. *J. Geophys. Res.* 87, 3893–3904.
- Anderson, D.L., Spetzler, H., 1970. Partial melting and the low-velocity zone. *Phys. Earth Planet. Inter.* 4, 62–64.
- Artemieva, I.M., 2009. The continental lithosphere: reconciling thermal, seismic, and petrologic data. *Lithos* 109, 23–46.
- Avé Lallemant, H.G., Mercier, J.-C.C., Carter, N.L., 1980. Rheology of the upper mantle: inference from peridotite xenoliths. *Tectonophysics* 70, 85–114.
- Barrell, J., 1914. The strength of the crust, Part VI. Relations of isostatic movements to a sphere of weakness – the asthenosphere. *J. Geol.* 22, 655–683.
- Beghein, C., Trampert, J., 2004. Probability density functions for radial anisotropy: implications for the upper 1200 km of the mantle. *Earth Planet. Sci. Lett.* 217, 151–162.
- Beghein, C., Trampert, J., van Heijst, H.J., 2006. Radial anisotropy in seismic reference models of the mantle. *J. Geophys. Res.* 111. doi:10.1029/2005JB003728.
- Bercovici, D., Karato, S., 2003. Whole mantle convection and transition-zone water filter. *Nature* 425, 39–44.
- Caristan, Y., 1982. The transition from high-temperature creep to fracture in Maryland diabase. *J. Geophys. Res.* 87, 6781–6790.
- Carlson, R.W., Pearson, D.G., James, D.E., 2005. Physical, chemical, and chronological characteristics of continental mantle. *Rev. Geophys.* 43. doi:10.1029/2004RG000156.
- Chen, S., Hiraga, T., Kohlstedt, D.L., 2006. Water weakening of clinopyroxene in the dislocation creep regime. *J. Geophys. Res.* 111. doi:10.1029/2005JB003885.
- Cooper, R.F., 2002. Seismic wave attenuation: energy dissipation in viscoelastic crystalline solids. In: Karato, S., Wenk, H.-R. (Eds.), *Plastic Deformation of Minerals and Rocks*. Mineralogical Society of America, Washington DC.

- Dai, L., Karato, S., 2009. Electrical conductivity of orthopyroxene: implications for the water content of the asthenosphere. *Proc. Jpn. Acad.* 85, 466–475.
- Dasgupta, R., Hirschmann, M.M., 2007. Effect of variable carbonate concentration on the solidus of mantle peridotite. *Am. Mineral.* 92, 370–379.
- Davies, G.F., 1988. Ocean bathymetry and mantle convection, 1. Large-scale flows and hotspots. *J. Geophys. Res.* 93, 10,467–10,480.
- Dziewonski, A.M., Anderson, D.L., 1981. Preliminary reference Earth model. *Phys. Earth Planet. Inter.* 25, 297–356.
- Eaton, D.W., Darbyshire, F., Evans, R.L., Grütter, H., Jones, A.G., Yuan, X., 2009. The elusive lithosphere–asthenosphere boundary (LAB) beneath cratons. *Lithos* 109, 1–22.
- Ekström, G., Dziewonski, A.M., 1998. The unique anisotropy of the Pacific upper mantle. *Nature* 394, 168–172.
- Faul, U.H., Jackson, I., 2005. The seismological signature of temperature and grain size variations in the upper mantle. *Earth Planet. Sci. Lett.* 234, 119–134.
- Fischer, K.M., Ford, H.A., Abt, D.L., Rychert, C.A., 2010. The lithosphere–asthenosphere boundary. *Ann. Rev. Earth Planet Sci.* 38, 551–575.
- Forsyth, W.D., 1975. The early structural evolution and anisotropy of the oceanic upper mantle. *Geophys. J. R. Astron. Soc.* 43, 103–162.
- Gaherty, J.B., Jordan, T.H., Gee, L.S., 1996. Seismic structure of the upper mantle in a central Pacific corridor. *J. Geophys. Res.* 101, 22291–22309.
- Ghahremani, F., 1980. Effect of grain boundary sliding on anelasticity of polycrystals. *Int. J. Solids Struct.* 16, 825–845.
- Green, D.H., Hibberson, W.O., Kovács, I., Rosenthal, A., 2010. Water and its influence on the lithosphere–asthenosphere boundary. *Nature* 467, 448–452.
- Gutenberg, B., 1926. Untersuchungen zur Frage, bis zu welcher Tiefe die Erde kristallin ist. *Z. Geophys.* 2, 24–29.
- Hernlund, J.W., Stevenson, D.J., Tackley, P.J., 2008a. Buoyant melting instabilities beneath extending lithosphere: 2. Linear analysis. *J. Geophys. Res.* 113. doi:10.1029/2006JB004863.
- Hernlund, J.W., Tackley, P.J., Stevenson, D.J., 2008b. Buoyant melting instabilities beneath extending lithosphere: 1. Numerical models. *J. Geophys. Res.* 113. doi:10.1029/2006JB004862.
- Hirano, N., Takahashi, E., Yamamoto, J., Abe, N., Ingle, S.P., Kaneoka, I., Hirata, T., Kimura, J.-I., Ishii, T., Ogawa, Y., Machida, S., Suyehiro, K., 2007. Volcanism in response to plate flexure. *Science* 313, 1426–1428.
- Hirschmann, M.M., 2006. Water, melting, and the deep Earth H₂O cycle. *Ann. Rev. Earth Planet Sci.* 34, 629–653.
- Hirschmann, M.M., 2010. Partial melt in the oceanic low velocity zone. *Phys. Earth Planet. Inter.* 179, 60–71.
- Hirschmann, M.M., Tenner, T., Aubaud, C., Withers, A.C., 2009. Dehydration melting of nominally anhydrous mantle: the primacy of partitioning. *Phys. Earth Planet. Inter.* 176, 54–68.
- Hirth, G., Kohlstedt, D.L., 1996. Water in the oceanic upper mantle – implications for rheology, melt extraction and the evolution of the lithosphere. *Earth Planet. Sci. Lett.* 144, 93–108.
- Hofmann, A.W., 1988. Chemical differentiation of the Earth: the relationship between mantle, continental crust, and oceanic crust. *Earth Planet. Sci. Lett.* 90, 297–314.
- Hofmann, A.W., 1997. Mantle geochemistry: the message from oceanic volcanism. *Nature* 385, 219–228.
- Hofmann, A.W., 2004. Sampling mantle heterogeneity through oceanic basalts: isotopes and trace elements. In: Holland, H.D., Turekian, K.K. (Eds.), *Treatise on Geochemistry*. Elsevier, Amsterdam.
- Holtzman, B.K., Kohlstedt, D.L., Zimmerman, M.E., Heidelbach, F., Hiraga, K., Hustoft, J., 2003. Melt segregation and strain partitioning: implications for seismic anisotropy and mantle flow. *Science* 301, 1227–1230.
- Jackson, I., 2009. Properties of rocks and minerals – physical origins of anelasticity and attenuation in rock. In: Schubert, G. (Ed.), *Treatise on Geophysics*. Elsevier, Amsterdam.
- Jackson, I., Faul, U.H., 2010. Grainsize-sensitive viscoelastic relaxation in olivine: towards a robust laboratory-based model for seismological application. *Phys. Earth Planet. Inter.* 183, 151–163.
- Jackson, I., Fitz Gerald, J.D., Faul, U.H., Tan, B.H., 2002. Grain-size sensitive seismic-wave attenuation in polycrystalline olivine. *J. Geophys. Res.* 107. doi:10.1029/2002JB001225.
- Jackson, I., Faul, U.H., Fitz Gerald, J.D., Tan, B., 2004. Shear wave attenuation and dispersion in melt-bearing olivine polycrystals: 1. Specimen fabrication and mechanical testing. *J. Geophys. Res.* 109. doi:10.1029/2003JB002406.
- Jacobsen, S.D., Jiang, F., Mao, Z., Duffy, T.S., Smyth, J.R., Holl, C.M., Frost, D.J., 2008. Effects of hydration on the elastic properties of olivine. *Geophys. Res. Lett.* 35. doi:10.1029/2008GL034398.
- Karato, S., 1977. *Rheological Properties of Materials Composing the Earth's Mantle*. Ph. D., University of Tokyo.
- Karato, S., 1984. Grain-size distribution and rheology of the upper mantle. *Tectonophysics* 104, 155–176.
- Karato, S., 1986. Does partial melting reduce the creep strength of the upper mantle? *Nature* 319, 309–310.
- Karato, S., 1993. Importance of anelasticity in the interpretation of seismic tomography. *Geophys. Res. Lett.* 20, 1623–1626.
- Karato, S., 2003. Mapping water content in Earth's upper mantle. In: Eiler, J.E. (Ed.), *Inside the Subduction Factory*. American Geophysical Union, Washington DC.
- Karato, S., 2008a. Deformation of Earth Materials: Introduction to the Rheology of the Solid Earth. Cambridge University Press, Cambridge.
- Karato, S., 2008b. Insights into the nature of plume–asthenosphere interaction from central Pacific geophysical anomalies. *Earth Planet. Sci. Lett.* 274, 234–240.
- Karato, S., 2010. Rheology of the deep upper mantle and its implications for the preservation of the continental roots: a review. *Tectonophysics* 481, 82–98.
- Karato, S., 2011. Water distribution across the mantle transition zone and its implications for global material circulation. *Earth Planet. Sci. Lett.* 301, 413–423.
- Karato, S., Jung, H., 1998. Water, partial melting and the origin of seismic low velocity and high attenuation zone in the upper mantle. *Earth Planet. Sci. Lett.* 157, 193–207.
- Karato, S., Bercovici, D., Leahy, G., Richard, G., Jing, Z., 2006. Transition zone water filter model for global material circulation: where do we stand? In: Jacobsen, S.D., van der Lee, S. (Eds.), *Earth's Deep Water Cycle*. American Geophysical Union, Washington DC.
- Karato, S., Jung, H., Katayama, I., Skemer, P.A., 2008. Geodynamic significance of seismic anisotropy of the upper mantle: new insights from laboratory studies. *Ann. Rev. Earth Planet Sci.* 36, 59–95.
- Kawakatsu, H., Kumar, P., Takei, Y., Shinohara, M., Kanazawa, T., Araki, E., Suyehiro, K., 2009. Seismic evidence for sharp lithosphere–asthenosphere boundaries of oceanic plates. *Science* 324, 499–502.
- Kê, T.S., 1947. Experimental evidence of the viscous behavior of grain boundaries in metals. *Phys. Rev.* 71, 533–546.
- Kohlstedt, D.L., 2002. Partial melting and deformation. In: Karato, S., Wenk, H.-R. (Eds.), *Plastic Deformation of Minerals and Rocks*. Mineralogical Society of America, Washington DC.
- Kumar, P., Kawakatsu, H., 2011. Imaging the seismic lithosphere–asthenosphere boundary of the oceanic plate. *Geochem. Geophys. Geosyst.* 12. doi:10.1029/2010GC003358.
- Kumar, P., Kind, R., Yuan, X., and Mechie, J., in press. USArray receiver function images of the LAB. *Seismological Research Letters*.
- Kushiro, I., 2001. Partial melting experiments on peridotite and origin of mid-ocean ridge basalt. *Ann. Rev. Earth Planet Sci.* 29, 71–107.
- Lambert, I.B., Wyllie, P.J., 1970. Low-velocity zone of the Earth's mantle: incipient melting caused by water. *Science* 169, 764–766.
- Lenardic, A., Moresi, L.N., 1999. Some thoughts on the stability of cratonic lithosphere: effects of buoyancy and viscosity. *J. Geophys. Res.* 104, 12747–12759.
- Long, M.D., Silver, P.G., 2009. Mantle flow in subduction systems: the slab flow field and implications for mantle dynamics. *J. Geophys. Res.* 114. doi:10.1029/2008JB006200.
- Manga, M., 1996. Mixing of heterogeneities in the mantle: effect of viscosity differences. *Geophys. Res. Lett.* 23, 403–406.
- McCarthy, C., Takei, Y., Hiraga, T., 2011. Experimental study of attenuation and dispersion over a broad frequency range: 2. The universal scaling of polycrystalline materials. *J. Geophys. Res.* 116. doi:10.1029/2011JB008384.
- McKenzie, D., Bickle, M.J., 1988. The volume and composition of melt generated by extension of the lithosphere. *J. Petrol.* 29, 625–679.
- McKenzie, D., Jackson, J.A., Priestley, K., 2005. Thermal structure of oceanic and continental lithosphere. *Earth Planet. Sci. Lett.* 233, 337–349.
- Mierdel, K., Keppler, H., 2004. The temperature dependence of water solubility in enstatite. *Contrib. Mineral. Petrol.* 148, 305–311.
- Mierdel, K., Keppler, H., Smyth, J.R., Langenhorst, F., 2007. Water solubility in aluminous orthopyroxene and the origin of Earth's asthenosphere. *Science* 315, 364–368.
- Montagner, J.-P., Tanimoto, T., 1990. Global anisotropy in the upper mantle inferred from the regionalization of phase velocities. *J. Geophys. Res.* 95, 4797–4819.
- Montagner, J.-P., Tanimoto, T., 1991. Global upper mantle tomography of seismic wave velocities and anisotropies. *J. Geophys. Res.* 96, 20337–20351.
- Morris, S.J.S., Jackson, I., 2009. Diffusionally assisted grain-boundary sliding and viscosity of polycrystals. *J. Mech. Phys. Solids* 57, 744–761.
- Nettles, M., Dziewonski, A.M., 2008. Radially anisotropic shear velocity structure of the upper mantle globally and beneath North America. *J. Geophys. Res.* 113. doi:10.1029/2006JB004819.
- Nishimura, C.E., Forsyth, D.W., 1989. The anisotropic structure of the upper mantle in the Pacific. *Geophys. J.* 96, 203–229.
- Ottino, J.M., 1989. *The Kinematics of Mixing: Stretching, Chaos, and Transport*. Cambridge University Press, New York.
- Plank, T., Langmuir, A.H., 1992. Effects of melting regime on the composition of the oceanic crust. *J. Geophys. Res.* 97, 19749–19770.
- Raj, R., Ashby, M.F., 1971. On grain boundary sliding and diffusional creep. *Metall. Trans.* 2, 1113–1127.
- Ribe, N.M., 1985. The generation and compaction of partial melts in the earth's mantle. *Earth Planet. Sci. Lett.* 73, 361–376.
- Ritzwoller, M.H., Shapiro, N.M., Zhong, S., 2004. Cooling history of the Pacific lithosphere. *Earth Planet. Sci. Lett.* 226, 69–84.
- Russo, R., Silver, P.G., 1994. Trench-parallel flow beneath the Nazca plate from seismic anisotropy. *Science* 263, 1105–1111.
- Rychert, C.A., Shearer, P.M., 2009. A global view of the lithosphere–asthenosphere boundary. *Science* 324, 495–498.
- Rychert, C.A., Shearer, P.M., 2011. Imaging the lithosphere–asthenosphere boundary beneath the Pacific using SS waveform modeling. *J. Geophys. Res.* 116. doi:10.1029/2010JB008870.
- Rychert, C.A., Fischer, K.M., Rodenay, S., 2005. A sharp lithosphere–asthenosphere boundary imaged beneath eastern North America. *Nature* 434, 542–545.
- Schmerr, N., in press. The Gutenberg discontinuity: Melt at the lithosphere–asthenosphere boundary. *Science*.
- Schubert, G., Froidevaux, C., Yuen, D.A., 1976. Oceanic lithosphere: thermal and mechanical structure. *J. Geophys. Res.* 81, 3525–3540.
- Shankland, T.J., O'Connell, R.J., Waff, H.S., 1981. Geophysical constraints on partial melt in the upper mantle. *Rev. Geophys. Space Phys.* 19, 394–406.
- Spiegelman, M., Elliott, T., 1993. Consequences of melt transport for uranium series disequilibrium in young lavas. *Earth Planet. Sci. Lett.* 118, 1–20.

- Stein, C.A., Stein, S., 1992. A model for the global variation in oceanic depth and heat flow with lithospheric age. *Nature* 359, 123–129.
- Stixrude, L., Lithgow-Bertelloni, C., 2005. Mineralogy and elasticity of the oceanic upper mantle: origin of the low-velocity zone. *J. Geophys. Res.* 110. doi:10.1029/2004JB002965.
- Stocker, R.L., Gordon, R.B., 1975. Velocity and internal friction in partial melts. *J. Geophys. Res.* 80, 4828–4836.
- Stolper, E.M., 1980. A phase diagram for mid-ocean ridge basalts: preliminary results and implications for petrogenesis. *Contrib. Mineral. Petrol.* 74, 13–27.
- Sundberg, M., Cooper, R.F., 2010. A composite viscoelastic model for incorporating grain boundary sliding and transient diffusion creep: correlating creep and attenuation responses for materials with a fine grain size. *Philos. Mag.* 90, 2817–2840.
- Takei, Y., 2002. Effect of pore geometry on V_p/V_s : from equilibrium geometry to crack. *J. Geophys. Res.* 107. doi:10.1029/2001JB000522.
- Tauzin, B., Debayle, E., Wittinger, G., 2010. Seismic evidence for a global low-velocity layer within the Earth's upper mantle. *Nat. Geosci.* 3, 718–721.
- Thybo, H., 2006. The heterogeneous upper mantle low velocity zone. *Tectonophysics* 416, 53–79.
- Thybo, H., Perchuc, E., 1997. The seismic 8° discontinuity and partial melting in continental mantle. *Science* 275, 1626–1629.
- Toramaru, A., Fujii, N., 1986. Connectivity of melt phase in a partially molten peridotite. *J. Geophys. Res.* 91, 9239–9252.
- Visser, K., Trampert, J., Lebedev, S., Kennett, B.L.N., 2008. Probability of radial anisotropy in the deep mantle. *Earth Planet. Sci. Lett.* 270, 241–250.
- Waff, H.S., Blau, J.R., 1979. Equilibrium fluid distribution in an ultramafic partial melts under hydrostatic stress conditions. *J. Geophys. Res.* 84, 6109–6114.
- Wang, D., Mookherjee, M., Xu, Y., Karato, S., 2006. The effect of water on the electrical conductivity in olivine. *Nature* 443, 977–980.
- Yang, Y., Forsyth, D.W., Weeraratne, D.S., 2007. Seismic attenuation near the East Pacific Rise and the origin of the low-velocity zone. *Earth Planet. Sci. Lett.* 258, 260–268.
- Yoshino, T., Nishihara, Y., Karato, S., 2007. Complete wetting of olivine grain boundaries by a hydrous melt near the mantle transition zone. *Earth Planet. Sci. Lett.* 256, 466–472.

Supplemental Materials I: Influence of anelasticity on seismic wave velocities

In most of high-temperature anelasticity measurement, a power law relationship between Q (Q^{-1} represents the fraction of elastic energy that is dissipated as heat) and frequency is observed, viz.,

$$Q \propto \omega^\alpha \quad (\text{SI-1})$$

where Q is the quality factor and ω is frequency, and α is a non-dimensional parameter (~ 0.3). Such a behavior can be explained by an absorption band model where the characteristic frequencies of anelastic relaxation is distributed in a certain frequency range. When anelasticity occurs, then seismic wave velocity is reduced. If seismic frequency is in this frequency range, then the velocity reduction and Q are related as,

$$\frac{\Delta V}{V} = \frac{1}{2} \cot \frac{\alpha\pi}{2} \cdot Q^{-1}. \quad (\text{SI-2})$$

With a commonly observed value of $\alpha \approx 0.3$ we have $\frac{\Delta V}{V} \approx Q^{-1}$. Thus if $Q=80$, then $\frac{\Delta V}{V} \approx 1\%$.

A quite different situation will arise when there is a high frequency peak outside of the absorption band. When seismic frequency is within the absorption band, then the high-frequency peak has little contribution to seismic wave attenuation but it does contribute to velocity reduction. Consequently, the velocity reduction observed at the

seismic frequency can be larger than that expected from the observed Q assuming the absorption band model (**Fig. 2**). Recently, (JACKSON and FAUL, 2010) reported evidence for a high frequency peak in olivine aggregates to cause a large velocity reduction, $\sim 4\%$. The absorption peak for 1 mm (1 cm) grain-size “dry” olivine occurs at $T \sim 1300$ K (~ 1450 K). This means that in the lithosphere shallower than 60-80 km where temperature is less than 1300-1400 K, seismic wave velocity is the unrelaxed velocity, whereas in the deep asthenosphere where temperature is higher than 1500 K, velocity will be the relaxed velocity, the difference being $\sim 4\%$ (the amplitude of velocity reduction depends on the grain geometry and grain-size distribution, see (LEE et al., 2011)). The depth and the magnitude of velocity drop predicted from this model roughly agree with the seismological observations (KAWAKATSU et al., 2009).

However, a purely thermal model is difficult to explain the sharpness of the LAB. According to (JACKSON and FAUL, 2010), a variation in temperature of ~ 200 K is needed to go from the unrelaxed to relaxed regime. At 60-80 km depth in the old oceanic lithosphere, the temperature gradient is ~ 5 -10 K/km (KARATO and JUNG, 1998). Therefore the width of the LAB with a purely thermal model will be 20-40 km that is wider than the seismological constraints (less than 10-15 km (KAWAKATSU et al., 2009)) (see **Fig. 3, 4**).

The high-frequency peak observed by (JACKSON and FAUL, 2010) is likely due to elastically accommodated grain-boundary sliding. For this mechanism, the peak frequency is given by (KË, 1947)

$$\omega_{gbs}(T, C_W) = \frac{M}{\eta_{gbs}(T, C_W)} \frac{\delta}{L} \quad (\text{SI-3})$$

where ω_{gbs} is the characteristic frequency of anelastic relaxation due to grain-boundary sliding, T is temperature, C_W is water content, M is elastic modulus, η_{gbs} is grain-boundary viscosity, δ is the thickness of grain-boundary, and L is grain-size. However, the relaxation strength, i.e., the magnitude of velocity reduction, is independent of grain-size as far as the geometry of grain-boundaries does not change with grain-size. The depth variation of the characteristic frequency comes mainly from the depth variation in grain-boundary viscosity. (JACKSON and FAUL, 2010) considered temperature effect, but like all other transport properties, grain-boundary viscosity also likely depends on the water content. Following the experimental results on other properties, I assume that grain-boundary viscosity depends on water content as $\eta_{gbs} \propto C_W^r$ (C_W : water content, r : a constant $r=1-2$ (KARATO, 2006)). Under this assumption,

$$\frac{\omega_{gbs}(T, C_W)}{\omega_{gbs}(T_o, C_W^o)} = \left(\frac{C_W}{C_W^o} \right)^r \exp \left[- \frac{H_{gbs}^*}{RT_o} \left(\frac{T_o}{T} - 1 \right) \right] \quad (\text{SI-4})$$

where $\omega_{gbs}(T, C_W)$ is the characteristic frequency at temperature T and water content C_W , T_o , C_W^o are the reference temperature and reference water content respectively, H_{gbs}^* is the activation enthalpy for grain-boundary sliding. Based on the study by (JACKSON and FAUL, 2010), I assume $H_{gbs}^* = 300 \pm 100$ kJ/mol. There is no direct experimental studies on the influence of water on grain-boundary sliding, but based on experimental studies on other properties (KARATO, 2006), I assume $r=0, 1$, and 2 ($r=0$

corresponds to a case of no water effect). The water content versus depth relation is based on (KARATO and JUNG, 1998).

Fig. 3 shows the results of calculated depth variation of characteristic frequency where I chose the reference temperature of $T_o = 1300$ K and reference the water content of $C_W^0 = 10^{-4}$ wt% (below this water content, the characteristic frequency becomes insensitive to the water content) at which $\omega_{gbs}(T_o, C_W^o) = 1$ Hz (JACKSON and FAUL, 2010). It is seen that the characteristic frequency moves from lower than seismic frequency in the shallow part (the lithosphere) to higher than seismic frequency in the deeper part (the asthenosphere). The transition depth is ~ 70 km (for the old oceanic mantle) but the sharpness and the exact depth depend on the sensitivity to water content, i.e., r . If there is no effect of water ($r=0$), the transition starts at ~ 80 km (this depth will depend on the age of the lithosphere) but the transition is too diffuse compared to the seismological constraints (KAWAKATSU et al., 2009). However, if the influence of water is assumed with $r=1-2$, the transition occurs at ~ 70 km and is sharp, consistent with the seismological observations. Although there are no direct experimental studies on the role of water on grain-boundary sliding nor grain-boundary diffusion, several related observations strongly suggest that transport properties of silicates are enhanced by water (COSTA and CHAKRABORTY, 2008; JUNG and KARATO, 2001; KARATO, 1989; NISHIHARA et al., 2006). (MCCARTHY et al., 2011) presented a model to support this hypothesis. Direct experimental study will be important to test this model.

Supplemental Materials II: slab-asthenosphere interaction in the subduction zone

Formation of a layer of accumulated melt (gabbro)

Melt is continuously produced in the upwelling current in the upper mantle. When melt reach the place where temperature is equal to the solidus, then melt freezes.

Therefore there will be a layer of frozen melt at the bottom of the lithosphere. As the lithosphere moves from the ridge, the thickness of this layer will increase.

Let w be the upwelling velocity, f be the average degree of melting (above the depth at which melt becomes buoyant), u_p the plate velocity and $h(x)$ be the thickness of such a layer at the place whose distance from the ridge is x . Then the mass balance requires

$$\frac{dh}{dx} = \frac{w}{u_p} f \quad (\text{SII-1})$$

and hence

$$h = \frac{w}{u_p} fx = wft \quad (\text{SII-2})$$

where t is the age of the plate ($x = u_p t$). If we use the following values, $w = 1$ mm/y (BERCOVICI and KARATO, 2003) and $f = 0.1-1$ %, then for the age of 100 Myrs, I get $h \sim 0.1-1$ km. This layer is too thin to cause a significant signal in the receiver function with a typical wavelength, but could be thick enough to lubricate the LAB as I will show in the next section. However, if the influence of small-scale convection is included, then

the thickness of the melt-rich layer will increase and it might become visible in the receiver function records (Parmentier, personal communication, 2011).

Decoupling caused by a thin weak layer at the bottom of the lithosphere

If we assume that the asthenospheric flow is driven mainly by the slab motion, then the asthenospheric flow below subducting slabs is strongly controlled by the nature of slab motion and the mechanical coupling between the slab and the asthenosphere. Let us consider that the slab sinks into the mantle with a velocity U but it also migrates normal to the trench with a velocity V (**Fig. SI**) ($V \ll U$ in most cases), and let us examine which component controls the flow in the asthenosphere.

When trench migration occurs, the trench parallel flow will occur in the asthenosphere due to the coupling via normal stress and its velocity can be calculated from the consideration of mass conservation as

$$HV \approx vL \quad (\text{SII-3})$$

where L is the length scale from the trench where the trench parallel flow occurs, H is the length of a trench (**Fig. SI**).

The flow in the asthenosphere also occurs due to coupling via shear stress. For homogeneous viscosity, the trench normal flow velocity caused by the slab with velocity U at a distance x from the slab caused by the shear stress by slab subduction is given by

$$\frac{u}{U} = 1 - \frac{x}{L}. \quad (\text{SII-4})$$

So near the trench, $u \approx U$. Therefore the ratio of trench parallel to trench normal flow velocities in the asthenosphere are given by

$$\frac{v}{u} \approx \frac{V}{U} \frac{H}{L} \approx \frac{V}{U} \ll 1 \quad (\text{SII-5})$$

where I use values of $V=1$ cm/y, $U=10$ cm/y, $L=5,000$ km and $H=5,000$ km for representative values.

Therefore if viscosity is homogeneous and subduction velocity is larger than trench migration velocity, then subduction velocity determines the velocity of asthenosphere motion below it. In order for trench parallel flow to dominate for a relative small trench migration velocity, the assumption of homogenous viscosity needs to be modified. If we introduce a thin low viscosity layer with a thickness δ and viscosity η_o , the degree of slab-asthenosphere coupling is reduced, and the equation (SII-4) for the flow outside of a weak zone will be modified to

$$\frac{u}{U} = \frac{\xi}{1+\xi} \left(1 - \frac{x}{L}\right) \quad (\text{SII-6})$$

where u is the velocity at a distance δ from the trench and

$$\xi = \frac{L}{\delta} \frac{\eta_o}{\eta} \quad (\text{SII-7})$$

where η is the viscosity of the asthenosphere away from the LAB. For the infinite viscosity at the boundary (or the zero width of the boundary) (i.e., $\xi \rightarrow \infty$), this relation goes back to (SII-4) whereas for a very low viscosity at the boundary (i.e., $\xi \ll 1$), it leads to $u \sim \xi U$ and the flow field caused by shear coupling is much weaker. Given $L / \delta \approx (0.5-1) \times 10^4$, ($L \sim 5,000-10,000$ km, $\delta \approx 1$ km), one needs $\eta_o / \eta < (1-2) \times 10^{-5}$ to bring $u/U < 0.1$.

Let us examine how small η_o / η could be for a physically reasonable process. (LONG and SILVER, 2009) invoked shear heating to reduce the viscosity near the LAB, but shear heating is highly unlikely to be efficient at the condition near the LAB because energy dissipation rate is so small there due to low viscosity (KARATO, 2008). An alternative mechanism to reduce the viscosity near the LAB is to assume the presence of frozen water-rich basaltic melt (wet gabbro). If partial melting occurs at 410-km, then upwelling materials continuously produce (a small amount of) melt. These melts have basaltic composition with a large amount of water (on the order of ~ 10 wt%). Once they reach the LAB, they will be frozen to form water-saturated gabbro. There are no detailed rheological studies on gabbro, and I use the result on the dislocation creep of clinopyroxene by (CHEN et al., 2006) as a first-order approximation. By comparing their results with the flow law of water-bearing olivine by (KARATO and JUNG, 2003), I find that the viscosity ratio at a constant stress at 1200-1300 K is $10^{-5}-10^{-6}$ for the water fugacity of 1-10 GPa ($\sim 10\%$ of saturation limit). If a melt-rich layer is present at the interface between the lithosphere and the asthenosphere, the viscosity contrast will be even smaller. Therefore the presence of a thin layer of (wet) gabbro (or a melt-rich layer) is a possible mechanism for decoupling.

- Bercovici, D. and Karato, S., 2003. Whole mantle convection and transition-zone water filter. *Nature* **425**, 39-44.
- Chen, S., Hiraga, T., and Kohlstedt, D. L., 2006. Water weakening of clinopyroxene in the dislocation creep regime. *Journal of Geophysical Research* **111**, 10.1029/2005JB003885.
- Costa, F. and Chakraborty, S., 2008. The effect of water on Si and O diffusion rates in olivine and implications for transport properties and processes in the upper mantle. *Physics of the Earth and Planetary Interiors* **166**, 11-29.
- Jackson, I. and Faul, U. H., 2010. Grainsize-sensitive viscoelastic relaxation in olivine: Towards a robust laboratory-based model for seismological application. *Physics of the Earth and Planetary Interiors* **183**, 151-163.
- Jung, H. and Karato, S., 2001. Effect of water on the size of dynamically recrystallized grains in olivine. *Journal of Structural Geology* **23**, 1337-1344.
- Karato, S., 1989. Grain growth kinetics in olivine aggregates. *Tectonophysics* **155**, 255-273.
- Karato, S., 2006. Influence of hydrogen-related defects on the electrical conductivity and plastic deformation of mantle minerals: A critical review. In: Jacobsen, S. D. and van der Lee, S. Eds.), *Earth's Deep Water Cycle*. American Geophysical Union, Washington DC.
- Karato, S., 2008. *Deformation of Earth Materials: Introduction to the Rheology of the Solid Earth*. Cambridge University Press, Cambridge.
- Karato, S. and Jung, H., 1998. Water, partial melting and the origin of seismic low velocity and high attenuation zone in the upper mantle. *Earth and Planetary Science Letters* **157**, 193-207.
- Karato, S. and Jung, H., 2003. Effects of pressure on high-temperature dislocation creep in olivine polycrystals. *Philosophical Magazine, A* **83**, 401-414.
- Kawakatsu, H., Kumar, P., Takei, Y., Shinohara, M., Kanazawa, T., Araki, E., and Suyehiro, K., 2009. Seismic evidence for sharp lithosphere-asthenosphere boundaries of oceanic plates. *Science* **324**, 499-502.
- Kê, T. S., 1947. Experimental evidence of the viscous behavior of grain boundaries in metals. *Physical Review* **71**, 533-546.
- Lee, L. C., Morris, S. J. S., and Wilkening, J., 2011. Stress concentrations, diffusionally accommodated grain boundary sliding and the viscoelasticity of polycrystals. *Proceedings of the Royal Society* **A467**, 1624-1644.
- Long, M. D. and Silver, P. G., 2009. Mantle flow in subduction systems: The subslab flow field and implications for mantle dynamics. *Journal of Geophysical Research* **114**, 10.1029/2008JB006200.
- McCarthy, C., Takei, Y., and Hiraga, T., 2011. Experimental study of attenuation and dispersion over a broad frequency range: 2. The universal scaling of polycrystalline materials. *Journal of Geophysical Research* **in press**.

Nishihara, Y., Shinmei, T., and Karato, S., 2006. Grain-growth kinetics in wadsleyite: effects of chemical environment. *Physics of Earth and Planetary Interiors* **154**, 30-43.

Fig. S1

A schematic drawing showing the geometry of subduction zone

Due to the presence of a thin weak layer (with a thickness δ), the motion in the asthenosphere below the subducting slab can be decoupled with plate subduction (velocity U), and could be controlled by trench migration (velocity V), if the viscosity there is much smaller than the viscosity in the general part of the asthenosphere. L : the length scale of convection (\sim plate size), H : the length of trench, δ : thickness of a weak layer

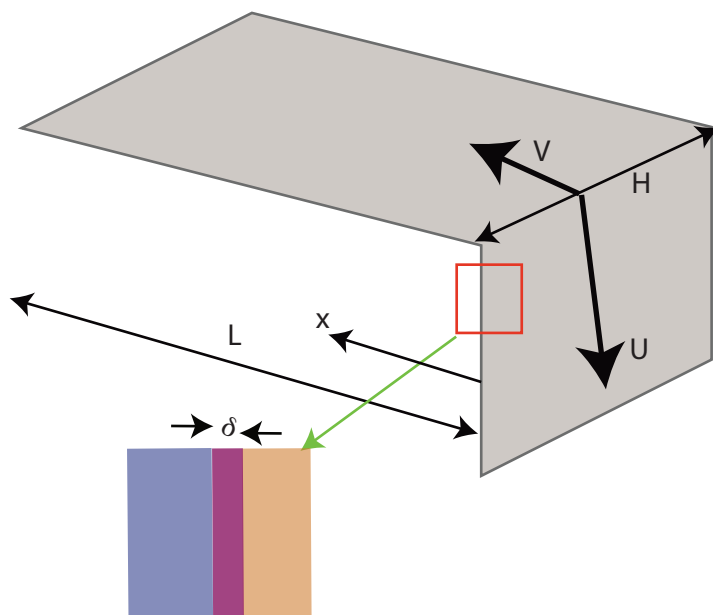


Fig. S1